# The Impact of IMRT and Proton Radiotherapy on Secondary Cancer Incidence

Uwe Schneider[1], Antony Lomax[2], Peter Pemler[1], Jürgen Besserer[1], Dieter Ross[1], Norbert Lombriser[1], Barbara Kaser-Hotz[3]

**Background and Purpose:** There is concern about the increase of radiation-induced malignancies with the application of modern radiation treatment techniques such as intensity-modulated radiotherapy (IMRT) and proton radiotherapy. Therefore, X-ray scatter and neutron radiation as well as the impact of the primary dose distribution on secondary cancer incidence are analyzed.
**Material and Methods:** The organ equivalent dose (OED) concept with a linear-exponential and a plateau dose-response curve was applied to dose distributions of 30 patients who received radiation therapy of prostate cancer. Three-dimensional conformal radiotherapy was used in eleven patients, another eleven patients received IMRT with 6-MV photons, and eight patients were treated with spot-scanned protons. The treatment plans were recalculated with 15-MV and 18-MV photons. Secondary cancer risk was estimated based on the OED for the different treatment techniques.
**Results:** A modest increase of 15% radiation-induced cancer results from IMRT using low energies (6 MV), compared to conventional four-field planning with 15-MV photons (plateau dose-response: 1%). The probability to develop a secondary cancer increases with IMRT of higher energies by 20% and 60% for 15 MV and 18 MV, respectively (plateau dose-response: 2% and 30%). The use of spot-scanned protons can reduce secondary cancer incidence as much as 50% (independent of dose-response).
**Conclusion:** By including the primary dose distribution into the analysis of radiation-induced cancer incidence, the resulting increase in risk for secondary cancer using modern treatment techniques such as IMRT is not as dramatic as expected from earlier studies. By using 6-MV photons, only a moderate risk increase is expected. Spot-scanned protons are the treatment of choice in regard to secondary cancer incidence.

**Key Words:** Organ equivalent dose · OED · Secondary cancer · Radiation carcinogenesis · IMRT · Proton radiotherapy

Strahlenther Onkol 2006;182:647–52
DOI 10.1007/s00066-006-1534-8

**Entstehung von Zweittumoren nach Radiotherapie: der Einfluss von IMRT und Protonentherapie**

**Hintergrund und Ziel:** Durch den Einsatz moderner Bestrahlungstechniken, wie intensitätsmodulierte Strahlentherapie (IMRT) und Protonentherapie, könnte die Anzahl strahleninduzierter Zweittumoren zunehmen. Deswegen wird der Einfluss von Röntgen- und Neutronenstreustrahlung (Tabelle 2) sowie der primären Dosisverteilung auf die Inzidenz von Sekundärtumoren quantifiziert.
**Material und Methodik:** Das Konzept der Organäquivalentdosis (OED) mit einer linear-exponentiellen und einer Plateau-Dosis-Wirkungs-Beziehung wurde auf die Dosisverteilungen von 30 Patienten mit Prostatakarzinom (Tabelle 1) angewendet. Von den 30 Patienten wurden elf mit konformaler Radiotherapie, elf mit 6-MV-IMRT und acht mit Protonentherapie („spot-scanned“) behandelt. Die Bestrahlungspläne wurden für 15-MV- und 18-MV-Photonen neu optimiert. Die OED für die verschiedenen Bestrahlungstechniken (Tabelle 3, Abbildung 1) ist proportional zur Sekundärtumorwahrscheinlichkeit.
**Ergebnisse:** Wird anstatt konventioneller Vier-Felder-Planung (15-MV-Photonen) ein 6-MV-IMRT-Plan verwendet, steigt die Anzahl strahleninduzierten Tumoren um etwa 15% an (Plateau-Dosis-Wirkungs-Beziehung: 1%). Wird allerdings eine höhere Photonenenergie für die IMRT verwendet (Abbildung 1), steigt die Wahrscheinlichkeit, einen Zweittumor zu entwickeln, um 20% für 15 MV bzw. um 60% für 18 MV an (2% bzw. 30% für eine Plateau-Dosis-Wirkungs-Beziehung). Verwendet man Protonentherapie („spot-scanned“) für die Behandlung, kann die Sekundärtumorinzidenz, unabhängig von der Dosis-Wirkungs-Beziehung, um 50% vermindert werden.
**Schlussfolgerung:** Wird neben der Streu- und Neutronenstrahlung auch die primäre Dosisverteilung in die Analyse der Sekundärtumorinzidenz mit einbezogen, steigt das Risiko für einen Zweittumor beim Einsatz der IMRT nicht so dramatisch an, wie in früheren Studien vorhergesagt. Verwendet man ausschließlich 6-MV-Photonen für die IMRT, wird das Sekundärtumorrisiko nur leicht erhöht. Der Einsatz der Protonentherapie kann in Bezug auf die Entstehung von Zweittumoren gegenüber der Photonentherapie von Vorteil sein.

**Schlüsselwörter:** Organäquivalentdosis · OED · Sekundärtumoren · Strahleninduzierter Krebs · IMRT · Protonentherapie

[1] Division of Medical Physics, Department of Radiation Oncology and Nuclear Medicine, Triemli Hospital, Zürich, Switzerland,
[2] Department of Radiation Medicine, Paul Scherrer Institute, Villigen, Switzerland,
[3] Division of Diagnostic Imaging and Radio-Oncology, Vetsuisse Faculty, University of Zürich, Switzerland. University Medical Center, NY, USA.

Received: October 13, 2005; accepted: August 3, 2006

## Introduction

In developed countries, more than half of all cancer patients receive radiotherapy at some stage in the management of their disease [7]. However, a radiation-induced secondary malignancy can be the price of success, if the primary cancer is cured or at least controlled [1, 2].

With the application of new radiation treatment modalities such as intensity-modulated radiotherapy (IMRT) or proton radiotherapy [20] increased cancer cure rates are expected. However, with the application of these treatment techniques also a larger number of secondary cancers is expected. The reason for this increased secondary malignancy incidence is the substantial increase in beam-on time of IMRT techniques to deliver the same target dose compared to conventional treatment techniques. In addition, during proton radiotherapy neutrons are created and could also have an impact on secondary cancer incidence.

Several attempts have been made to estimate the risk of secondary cancer development after radiation therapy. One strategy is to estimate these risks based on measured X-ray and neutron leakage and computing the effective dose [3, 5, 8, 19]. Estimates of the rate of induction of secondary malignancies can then be obtained by using published risk data such as the ICRP recommendations. Such estimates usually result in an extremely high risk of secondary cancers after IMRT. The risk estimates vary between 2 to 8 depending on technique and energy compared to conventional radiotherapy. The drawback of these studies is the fact that the impact of the primary dose field is totally neglected and, hence, the estimate of the risk increase could be far too large.

Another strategy is the estimation of cancer risk from the three-dimensional (3-D) dose distributions by applying radiation protection concepts including a cutoff dose to account for the reduced cancer risk at high dose [6, 11, 15].

**Table 1.** Treatment technique and prescribed dose listed for all 30 analyzed patients irradiated for prostate carcinoma. For photons also the treated MUs and for protons the number of applied protons are listed. CT: computed tomography; 3-D: three-dimensional conformal radiotherapy; IMRT: intensity-modulated radiotherapy; PRO: proton radiotherapy.

**Tabelle 1.** Bestrahlungstechniken und verschriebene Dosen für alle 30 Patienten mit Prostatakarzinom. Für die Photonenpläne ist auch die Anzahl der bestrahlten MUs und für die Protonenpläne die Anzahl der verwendeten Protonen aufgelistet. CT: Computertomographie; 3-D: dreidimensionale konformale Radiotherapie; IMRT: intensitätsmodulierte Radiotherapie; PRO: Protontherapie.

| Technique – patient # | Number of fields | Energy (MeV) | Prescribed dose (Gy/CGE) | Total applied MU 6 MV | Total applied MU 15 MV | Total applied MU 18 MV | Number of protons × $10^{-7}$ | CT volume $V_{CT}$ ($cm^3$) |
|---|---|---|---|---|---|---|---|---|
| 3-D – 1 | 4 | 15 | 76 | – | 9,888 | 8,753 | – | 14,646 |
| 3-D – 2 | 4 | 15 | 76 | – | 9,278 | 8,770 | – | 8,584 |
| 3-D – 3 | 4 | 15 | 76 | – | 9,667 | 9,037 | – | 20,978 |
| 3-D – 4 | 4 | 15 | 76 | – | 9,666 | 8,990 | – | 17,462 |
| 3-D – 5 | 4 | 15 | 76 | – | 9,542 | 8,974 | – | 10,498 |
| 3-D – 6 | 4 | 15 | 76 | – | 9,820 | 9,176 | – | 25,935 |
| 3-D – 7 | 4 | 15 | 76 | – | 9,897 | 9,678 | – | 19,914 |
| 3-D – 8 | 4 | 15 | 72 | – | 8,919 | 8,330 | – | 9,485 |
| 3-D – 9 | 4 | 15 | 72 | – | 8,913 | 8,462 | – | 11,160 |
| 3-D – 10 | 4 | 15 | 72 | – | 9,448 | 8,955 | – | 17,700 |
| 3-D – 11 | 4 | 15 | 67 | – | 8,663 | 8,096 | – | 22,248 |
| IMRT – 1 | 5 | 6 | 76 | 15,846 | 12,844 | 12,806 | – | 16,151 |
| IMRT – 2 | 5 | 6 | 76 | 19,076 | 15,276 | 15,162 | – | 8,584 |
| IMRT – 3 | 5 | 6 | 76 | 14,136 | 12,122 | 11,666 | – | 11,861 |
| IMRT – 4 | 5 | 6 | 72 | 26,892 | 23,400 | 16,164 | – | 12,231 |
| IMRT – 5 | 5 | 6 | 70 | 22,155 | 16,065 | 15,855 | – | 15,373 |
| IMRT – 6 | 5 | 6 | 76 | 14,706 | 11,704 | 12,008 | – | 15,355 |
| IMRT – 7 | 5 | 6 | 72 | 15,588 | 12,528 | 12,204 | – | 32,155 |
| IMRT – 8 | 5 | 6 | 72 | 15,660 | 13,068 | 12,528 | – | 11,517 |
| IMRT – 9 | 5 | 6 | 72 | 15,948 | 12,240 | 11,736 | – | 20,730 |
| IMRT – 10 | 5 | 6 | 76 | 16,454 | 12768 | 12,958 | – | 29,264 |
| IMRT – 11 | 5 | 6 | 72 | 20,628 | 17,892 | 18,324 | – | 10,933 |
| PRO – 1 | 2 | 214 | 74 | – | – | – | 9,140 | 10,003 |
| PRO – 2 | 2 | 214 | 74 | – | – | – | 5,191 | 12,422 |
| PRO – 3 | 2 | 214 | 74 | – | – | – | 4,742 | 10,239 |
| PRO – 4 | 2 | 214 | 74 | – | – | – | 4,020 | 11,187 |
| PRO – 5 | 2 | 214 | 74 | – | – | – | 7,870 | 9,142 |
| PRO – 6 | 2 | 214 | 74 | – | – | – | 6,000 | 13,188 |
| PRO – 7 | 2 | 214 | 74 | – | – | – | 11,320 | 8,914 |
| PRO – 8 | 2 | 214 | 74 | – | – | – | 7,224 | 9,965 |

Such approaches work not well for doses > 2–4 Gy and therefore the results from these studies must be interpreted with caution.

In this report, we apply the concept of organ equivalent dose (OED) to dose-volume histograms (DVHs) of patients treated for prostatic carcinoma with 3-D conformal radiotherapy, IMRT, and proton radiotherapy. Any dose distribution in an organ is equivalent and corresponds to the same OED, if it causes the same radiation-induced cancer incidence [16]. For low doses the OED is simply average organ dose, and hence the dose-response relationship for cancer induction here is with good precision a linear function of dose. However, for high doses a dose-response relationship extracted from secondary cancer incidence data after radiotherapy of Hodgkin's disease is used [14].

We believe that the application of the OED concept to analyze 3-D dose distributions gives more realistic estimates of the potential risk for secondary cancer induction after the clinical application of different radiotherapy techniques.

## Material and Methods

### Patients

The patient treatments analyzed in this study consisted of 30 patients irradiated for prostatic carcinoma. Eleven patients received 3-D conformal radiotherapy with a conventional four-field treatment technique using 15-MV photons delivered by a Varian Clinac CL2300 (Varian Medical Systems, Palo Alto, USA) in three phases and 1.8-Gy fractions. Another eleven patients were treated with IMRT and five irradiation fields using 6-MV photons using a sliding MLC (multileaf collimator) and a simultaneous boost technique with 2.0-Gy fractions. Both groups of patients were irradiated at the Triemli Hospital Zürich, Switzerland, with a Varian Clinac CL2300. The treatment plans of these patients were recalculated with 15-MV and 18-MV photons, respectively. Finally, eight patients were irradiated with two lateral fields using spot-scanned protons. The latter patients were treated at the proton radiotherapy beam line at the Paul Scherrer Institute (PSI), Villigen, Switzerland, with a dose of 2.0 CGE (cobalt-gray equivalent) per fraction which is 1.8 Gy assuming an RBE (relative biological effectiveness) of 1.1. An overview of the analyzed patients is given in Table 1 where also the prescribed dose is listed. Patients were chosen such that the average prescribed dose was similar in each group (3-D conformal radiotherapy: 73.8 Gy; IMRT: 73.6 Gy; protons: 74 CGE).

### Volume Definition

The total volume of a patient was divided into the volume included in the CT (computed tomography) scan ($V_{CT}$) and the volume not scanned ($Vno_{CT}$). We define $Vno_{CT}$ by assuming a reference body weight of 70 kg and a reference specific gravity of 1.07 [9, 20]:

$$V_{noCT} = \frac{70{,}000}{1.07}\ cm^3 - V_{CT} \quad (1).$$

### Photons

We calculated the photon dose distributions using Eclipse 7.3.10 (Varian Medical Systems, Palo Alto, USA). Differential DVHs of $V_{CT}$ were calculated from the 3-D dose distributions. For $Vno_{CT}$, a homogeneous dose bath of phantom scatter, collimator scatter and neutron dose was assumed. It is assumed that collimator scatter, including leakage dose $D_{col}^{X}$ and phantom scatter $D_{pha}^{X}$ contribute equally to the total photon scatter dose [17]. The photon scatter dose was estimated from measured data for a point located 50 cm away from the center of a 10 × 10 cm² treatment field at 10 cm depth and is listed in Table 2 for all photon energies [17]. Measured data on neutron dose from medical electron accelerators were taken from d'Errico et al. [4]. They measured the neutron dose equivalent for 15-MV and 18-MV photons at three different depths in water in the center of a 10 × 10 cm² field and 50 cm off axis. For our estimates, we used the measured neutron equivalent dose values at 5 cm depth, since this corresponds approximately to the average neutron dose in depth (Figure 5 of [4]). The neutron dose equivalents $D_{axis}^{N}$ and $D_{off\text{-}axis}^{N}$ are listed in Table 2.

The 3-D conformal and IMRT photon dose distributions $D_{CT}^{3D/IMRT}$ in $V_{CT}$ which were computed with the treatment-planning system were then corrected for photon scatter and neutron dose:

$$D_{CT}^{3D/IMRT} = D_{TPS}^{3D/IMRT} + D_{axis}^{N} \quad (2).$$

In $V_{noCT}$, the homogeneous dose for the 3-D conformal treatments is

$$D_{noCT}^{3D} = (D_{col}^{X} + D_{pha}^{X})MU^{3D} + D_{off\text{-}axis}^{N} \quad (3),$$

where $MU^{3D}$ are the applied monitor units from Table 1. For the IMRT plans, the same amount of phantom scatter as in the 3-D conformal plans was assumed. However, collimator scat-

**Table 2.** X-ray phantom scatter $D_{pha}^{X}$ [14], collimator scatter and leakage $D_{col}^{X}$ [14], and neutron dose equivalent in Sv per treated MU for photons [4] and per treatment proton for proton radiotherapy [12].

**Tabelle 2.** Röntgenstreustrahlung (Phantomstreuung $D_{pha}^{X}$ [14]; Kollimatorstreuung und Leckstrahlung $D_{col}^{X}$ [14]) sowie Neutronenäquivalentdosis in Sv pro bestrahlte MU für Photonen [4] und pro bestrahltes Proton für Protonentherapie [12].

| Radiation type | 6-MV photons | 15-MV photons | 18-MV photons photons | Protons |
|---|---|---|---|---|
| X-ray phantom scatter: $D_{pha}^{X}$ | $2 \times 10^{-6}$ | $3 \times 10^{-6}$ | $3 \times 10^{-6}$ | – |
| X-ray collimator scatter and leakage: $D_{col}^{X}$ | $2 \times 10^{-6}$ | $3 \times 10^{-6}$ | $3 \times 10^{-6}$ | – |
| Neutrons on central axis: $D_{axis}^{N}$ | 0 | $1 \times 10^{-5}$ | $4 \times 10^{-5}$ | $6 \times 10^{-14}$ |
| Neutrons 50 cm off axis: $D_{off\text{-}axis}^{N}$ | 0 | $1 \times 10^{-6}$ | $1 \times 10^{-5}$ | $2.5 \times 10^{-14}$ |

ter is produced throughout the whole irradiation time und must be weighted with the monitor units $MU^{IMRT}$ applied through IMRT:

$$D_{noCT}^{IMRT} = D_{col}^{X}\, MU^{IMRT} + D_{pha}^{X}\, MU^{3D} + D_{off\text{-}axis}^{N} \quad (4).$$

### Protons

Proton dose was computed using the PSI proton treatment-planning program [10, 12]. Differential DVHs of $V_{CT}$ were calculated from the 3-D dose distributions. Neutron dose was estimated using the measurements of Schneider et al. [13]. They measured neutron dose equivalent during proton radiotherapy using spot-scanned protons and obtained a mean dose of $6 \times 10^{-14}$ Sv/proton in the target and $2.5 \times 10^{-14}$ Sv/proton in the patient volume excluding the target. Total neutron equivalent dose for the different treatment plans was then computed by multiplying these values by the number of applied protons for the different treatment plans which are listed in Table 1. The 3-D dose distribution $D_{CT}^{PRO}$ in $V_{CT}$ is then

$$D_{CT}^{PRO} = D_{TPS}^{PRO} + D_{axis}^{N} \quad (5).$$

The homogeneous dose inside $V_{noCT}$ is estimated as

$$D_{noCT}^{PRO} = D_{no\text{-}axis}^{N} \quad (6).$$

### OED and Risk Calculation

The dose-response relationship for radiation-induced cancer is not very well known for doses > 2 Gy. There are two extreme possibilities for the shape of the dose-response curves at high dose, a linear-exponential and a plateau curve [6]. It can be confidently expected that the real dose-response for cancer induction lies between these extreme cases [6]. Therefore, in the following we use both possibilities to estimate secondary cancer risk.

By using the concept of OED for the whole body volume, the cancer incidence is directly proportional to OED:

$$I = I_0 \times OED \quad (7),$$

where $I$ is the secondary cancer incidence for solid cancers and $I_0$ is the radiation-induced cancer risk for low dose from the atomic bomb survivors. It should be noted here, that all population-related parameters, as, for example, age at exposure, attained age and sex are included in $I_0$. Therefore, a comparison of treatment plans with respect to second cancer incidence for one patient or a group of patients of the same population, can be performed simply by comparing the corresponding *OEDs*.

For the CT volume $V_{CT}$ where the dose is inhomogeneously distributed and a DVH was obtained, the OED was calculated [16] as

$$OED_{CT} = \frac{1}{(V_{CT} + V_{noCT})} \sum_i DVH\,(D_{CT}^{i})\, D_{CT}^{i}\, e^{-\alpha D_{CT}^{i}} \quad (8),$$

where $DVH(D_{CT}^{i})$ is the volume which corresponds to the dose $D_{CT}^{i}$. We assumed here a linear-exponential dose-response relation using a model parameter $\alpha = 0.08\ Gy^{-1}$ [16, 18].

For a plateau dose-response relationship with a model parameter $\delta = 0.24\ Gy^{-1}$, the OED is

$$OED_{CT} = \frac{1}{(V_{CT} + V_{noCT})} \sum_i DVH\,(D_{CT}^{i})\,(1 - e^{-\delta D_{CT}^{i}})/\delta \quad (9).$$

In $V_{noCT}$ we assume scatter dose and neutron dose homogeneously distributed in the patient and can write for the linear-exponential dose-response curve

$$OED_{noCT} = \frac{V_{noCT}}{V_{CT} + V_{noCT}}\, D_{noCT}\, e^{-\alpha D_{noCT}} \quad (10)$$

and

$$OED_{noCT} = \frac{V_{noCT}}{V_{CT} + V_{noCT}}\, D_{noCT}\,(1 - e^{-\delta D_{noCT}})/\delta \quad (11)$$

using a plateau dose-response relationship, respectively.

The risk for the occurrence of a secondary cancer after treatment with radiation is then proportional to the sum of the OED inside and outside of the CT, respectively:

$$I \approx \left(OED_{CT} + OED_{noCT}\right) \quad (12).$$

## Results

### 3-D Conformal Therapy

The obtained OED for both the linear-exponential and plateau dose-response with the corresponding standard deviation (variation between the different patients) is listed in Table 3 and plotted in Figure 1. It is interesting to note that for conventional 3-D conformal dose planning with 15 MV nearly *85%* of the OED comes from the primary dose contribution and only the remaining *15%* from X-ray scatter and neutrons.

### IMRT

The *OED* for the IMRT treatment plans is increased compared to the conventional *four*-field conformal treatments (Table 3). For the *6-MV* IMRT plan the increase is close to *15%* using the linear-exponential dose-response (*1%* for the plateau dose-response). The part originating from X-ray and neutron scatter is decreased, since at such low photon energies nearly no neutrons are produced. However, the OED resulting from the primary dose field is increased by *25%*, as during IMRT the volume receiving low dose is significantly higher. IMRT treatment plans with *15-MV* and *18-MV* photons have a *20%* and *60%* increased risk compared to the 3-D conformal plans. It should be noted, that for *15 MV* and *18 MV* the risk originating from the primary dose is less than the risk from the *6-MV* IMRT plan, because of the advantageous depth dose properties when using the higher energy. However, the neutron dose contribution is remarkably increased when using higher photon energies for IMRT.

### Proton Therapy

The use of spot-scanned protons reduces, independent of the dose-response curve used, the secondary cancer risk after

prostate therapy by a factor of 2 compared to the 3-D conformal treatment plans. Although the neutron contribution is nearly as large as for the *15-MV* IMRT plans, the dose advantage from the superior proton depth dose characteristics is reducing the risk resulting from the primary dose by *> 60%*.

**Tables 3a and 3b.** Organ equivalent dose (OED) for different prostate radiation treatment techniques; a) for a linear-exponential and b) for a plateau dose-response relationship. 3-D: three-dimensional conformal radiotherapy; IMRT: intensity-modulated radiotherapy.

**Tabellen 3a und 3b.** Organäquivalentdosis (OED) für verschiedene Bestrahlungstechniken der Prostata; a) für eine linear-exponentielle und b) für eine Plateau-Dosis-Wirkungs-Beziehung. 3-D: dreidimensionale konformale Radiotherapie; IMRT: intensitätsmodulierte Radiotherapie.

| Treatment technique | OED – primary dose (Gy) | OED – X-ray scatter and neutrons (Sv) | OED – total (Gy) | $\sigma_{OED}$ (Gy) |
|---|---|---|---|---|
| a) Linear-exponential dose-response | | | | |
| 3-D, 15 MV | 0.33 | 0.06 | 0.40 | 0.09 |
| 3-D, 18 MV | 0.33 | 0.16 | 0.49 | 0.09 |
| IMRT, 6 MV | 0.42 | 0.04 | 0.46 | 0.10 |
| IMRT, 15 MV | 0.39 | 0.09 | 0.48 | 0.09 |
| IMRT, 18 MV | 0.40 | 0.23 | 0.63 | 0.10 |
| Protons | 0.13 | 0.08 | 0.21 | 0.04 |
| b) Plateau dose-response | | | | |
| 3-D, 15 MV | 0.44 | 0.06 | 0.50 | 0.12 |
| 3-D, 18 MV | 0.42 | 0.15 | 0.57 | 0.12 |
| IMRT, 6 MV | 0.47 | 0.04 | 0.51 | 0.11 |
| IMRT, 15 MV | 0.42 | 0.09 | 0.51 | 0.09 |
| IMRT, 18 MV | 0.43 | 0.22 | 0.65 | 0.10 |
| Protons | 0.16 | 0.08 | 0.24 | 0.06 |

## Discussion and Conclusion

The results found in this study imply that IMRTs are related to an increased risk of secondary tumor induction. However, compared to previous publications on this topic [5, 19], we found only a moderate increase of around *15%* for prostate radiotherapy when a patient is treated with a *6-MV* IMRT plan instead of a conventional *15-MV four*-field plan. Our findings seem to be in contradiction to a recent publication of Followill et al. [5]. They found, for example, for *18-MV* photons a *280%* difference between radiation-induced malignancies from conventional radiation treatment compared to IMRT. One explanation for this is that Followill et al. [5] analyzed exclusively scattered X-ray and neutron radiation. However, they did not include the impact of the primary radiation field on radiation-induced cancer. The primary radiation field is responsible for the major part of radiation-induced cancers. Therefore, we believe that a fair comparison of radiation-induced cancers resulting from different radiation treatment techniques must include the impact of the primary radiation field as well. For a conservative comparison with the Followill data the linear-exponential dose-response relationship should be used, which gives highest weight to the scatter radiation.

The usage of larger photon energies than *15 MV* for IMRT can result in a significantly larger neutron component. For

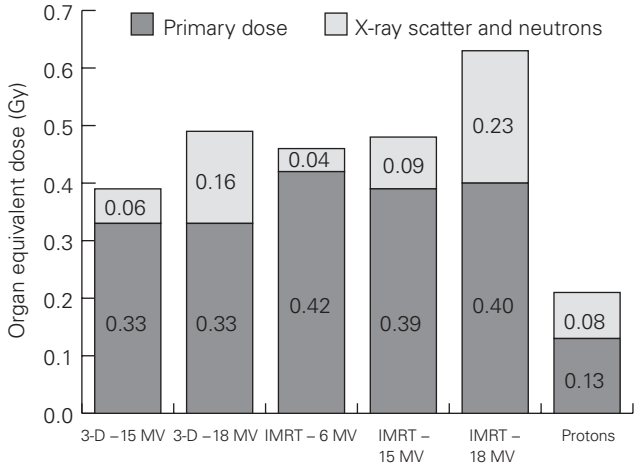


**Figure 1a – Abbildung 1a**

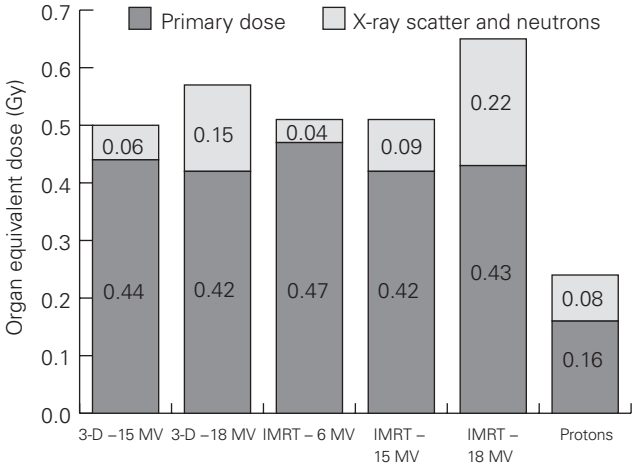


**Figure 1b – Abbildung 1b**

**Figures 1a and 1b.** OED for different treatment techniques applied to prostate radiotherapy; a) for a linear-exponential, and b) for a plateau dose-response relationship.

**Abbildungen 1a und 1b.** OED für verschiedene Bestrahlungstechniken der Prostata; a) für eine linear-exponentielle und b) für eine Plateau-Dosis-Wirkungs-Beziehung.

*18-MV* photons the dose from X-ray scatter and neutrons is approximately *two to three* times larger than compared to *15-MV* [4, 21]. It can be estimated that IMRT planned with 18 MV would result in a *60%* increased risk compared to the 3-D conformal plan and approximately a *30%* increased risk compared to the *15-MV* IMRT plan. As a consequence, to reduce the risk, always the smallest possible photon energy should be chosen for IMRT.

It should be noted that the low cancer incidence after proton radiotherapy is a consequence of the low neutron contamination of the spot-scanning technique which requires no scattering, collimation or compensation, all of which could increase it up to a factor of 10 dependent on the specific beam line design.

In this work we have looked at several cases but only investigated one indication (prostate cancer). It is clearly difficult to draw general conclusions and extrapolate these findings to other indications. However, as the major part to the risk of secondary cancer incidence results from the primary dose distribution, the findings of this work should also be applicable to other indications. This needs to be confirmed by performing similar calculations for other indications.

### References


1. Bray F, Sankila R, Ferlay J, et al. Estimates of cancer incidence and mortality in Europe in 1995. Eur J Cancer 2002;38:99–166.
2. Brenner DJ, Curtis RE, Hall EJ, et al. Second malignancies in prostate carcinoma patients after radiotherapy compared with surgery. Cancer 2002; 88:398–406.
3. Cumberlin RL, Dritschilo A, Mossman KL. Carcinogenic effects of scattered dose associated with radiation therapy. Int J Radiat Oncol Biol Phys 1989; 17:623–9.
4. D'Errico F, Luszik-Bhadra M, Nath R, et al. Depth dose-equivalent and effective energies of photoneutrons generated by 6–18 MV X-ray beams for radiotherapy. Health Phys 2001;80:4–11.
5. Followill D, Geis P, Boyer A. Estimates of whole-body dose equivalent produced by beam intensity modulated conformal therapy [Erratum in: Int J Radiat Oncol Biol Phys 1997;39:783]. Int J Radiat Oncol Biol Phys 1997; 38:667–72.
6. Gershkevitsh E, Clark CH, Staffurth J, et al. Dose to bone marrow using IMRT techniques in prostate cancer patients. Strahlenther Onkol 2005;181:172–8.
7. Hall EJ. Henry S. Kaplan Distinguished Scientist Award 2003. The crooked shall be made straight; dose-response relationships for carcinogenesis. Int J Radiat Biol 2004;80:327–37.
8. Hall EJ, Wuu CS. Radiation-induced second cancers: the impact of 3D-CRT and IMRT. Int J Radiat Oncol Biol Phys 2003;56:83–8.
9. ICRP Publication 23. Report on the Task Group on Reference Man. London: Pergamon Press, 1975.
10. Lomax AJ, Pedroni E, Schaffner B, et al. 3D treatment planning for conformal proton therapy by spot scanning. In: Faulkner K, Carey B, Crellin A, et al., eds. Quantitative imaging in oncology. London: BIR, London, 1996:67–71.
11. Miralbell R, Lomax A, Cella L, et al. Potential reduction of the incidence of radiation-induced second cancers by using proton beams in the treatment of pediatric tumors. Int J Radiat Oncol Biol Phys 2002;54:824–9.
12. Rutz HP, Lomax AJ. Donut-shaped high-dose configuration for proton beam radiation therapy. Strahlenther Onkol 2005;181:49–53.
13. Schneider U, Agosteo S, Pedroni E, et al. Secondary neutron dose during proton therapy using spot scanning. Int J Radiat Oncol Biol Phys 2002; 53:244–51.
14. Schneider U, Kaser-Hotz B. A simple dose-response relationship for modelling secondary cancer incidence after radiotherapy. Z Med Phys 2005; 15:31–7.
15. Schneider U, Lomax A, Lombriser N. Comparative risk assessment of secondary cancer incidence after treatment of Hodgkin's disease with photon and proton radiation. Radiat Res 2000;154:382–8.
16. Schneider U, Zwahlen D, Ross D, et al. Estimation of radiation-induced cancer from 3D-dose distributions: concept of organ equivalent dose. Int J Radiat Oncol Biol Phys 2005;61:1510–5.
17. Stovall M, Blackwell CR, Cundiff J, et al. Fetal dose from radiotherapy with photon beams: report of AAPM Radiation Therapy Committee Task Group No. 36. Med Phys 1995;22:63–82.
18. UNSCEAR. Report to the General Assembly. Sources and effects of ionizing radiation, vol II: Effects, Annex I: Epidemiological evaluation of radiation-induced cancer. New York: UNSCEAR, 2000 (*http://www.unscear.org/reports/2000_2.html*).
19. Verellen D, Vanhavere F. Risk assessment of radiation-induced malignancies based on whole-body equivalent dose estimates for IMRT treatment in the head and neck region. Radiother Oncol 1999;53:199–203.
20. Villeirs GM, Van Vaerenbergh K, Vakaet L, et al. Interobserver delineation variation using CT versus combined CT + MRI in intensity-modulated radiotherapy for prostate cancer. Strahlenther Onkol 2005;181:424–30.
21. Wittig A, Moss RL, Stecher-Rasmussen F, et al. Neutron activation of patients following boron neutron capture therapy of brain tumors at the high flux reactor (HFR) Petten (EORTC Trials 11961 and 11011). Strahlenther Onkol 2005;181:774–82.



**Address for Correspondence**
Uwe Schneider, PhD
Division of Medical Physics
Department of Radiation Oncology and Nuclear Medicine
Triemli Hospital Zürich
8063 Zürich
Switzerland
Phone (+41/44) 4662-432, Fax -706
e-mail: uwe.schneider@psi.ch